Investigation of liquid phase characteristics in an inclined open microchannel

Antonios D. ANASTASIOU [1], Asterios GAVRIILIDIS[2], Aikaterini A. MOUZA[1*]

* Corresponding author: Tel.:+302310994161; Fax:+302310996209; Email: mouza@cheng.auth.gr
[1] Department of Chemical Engineering, Aristotle University of Thessaloniki, Greece
[2] Department of Chemical Engineering, UCL, UK

Abstract. An important variable in the designing of gas-liquid reactors is the interfacial area available for the conduction of the two phases. Falling film microreactors (*FFMR*) are devices which can offer extended specific surfaces (up to 20,000m^2/m^3) and for this reason they are used in many multiphase processes. The aim of this work is to assess the effect of the microchannel width as well as the flow rate and the physical properties of the liquid phase on the geometrical characteristics (i.e. thickness and surface shape) of the liquid film, which were measured using Micro Particle Image Velocimetry (*μ-PIV*). The experiments were conducted in single microchannels with widths of 1200, 600 and 300μm and for Reynolds numbers between 0.9 and 39.7, while water and aqueous solutions of glycerol and butanol were used as working fluids. It was also verified that a common expression for predicting film thickness in macroscale is not applicable in microscale.

Keywords: Micro reactor, Falling film, *μ*-PIV, Liquid meniscus

1. Introduction

Microfluidics covers a large variety of applications, e.g., detection and control of chemical reactions, sample preparation, flow and pressure sensors, microequipment for mixing, separation or heating, microscale systems for biological diagnostics as *DNA* analysis, pumping systems (Nguyen and Wereley, 2002). Microsystems are characterized by low consumption of reagents, quick system response as well as multifunctionality, since various unit operations can be combined in a single piece of equipment. Thus, in an effort to build more compact, smaller, cheaper and more efficient equipment many micro-systems have been developed.

There are several differences in physical behavior observed between macro and micro systems which can be best explained by considering the different forces that govern the flow. Due to the small characteristic dimension of the conduit, viscous forces dominate the flow, while inertial forces become less important. In the same time the ratio of surface area to system volume increases and so does the relative importance of surface forces. Additionally, as interfacial area is greater, heat and mass transfer rates are enhanced.

Of great interest in microfluidics is the study of multiphase flow in microchannels. The liquid and gas phase can be either dispersed or separated. Although in both cases high specific areas can be obtained, in falling film microreactors (*FFMR*) a stable and well controlled interface is assured (Ziegenbalg et al., 2010). In microchannels the film is quite stable and might have a thickness of less than 100μm, while in conventional falling film systems the film thickness is between 0.5 and 3mm. As such thin films offer high heat and mass transfer capabilities, *FFMR* are suitable for many applications (e.g reaction, extraction, evaporation and highly exothermic processes). The majority of the published work concerning *FFMR* deals with the conversion rate of specific reactions, [e.g. Chambers et al., (2001), Chasanis et al., (2009), Stavarek et al., (2009)], while little work has been published on the characteristics of the interface in such devices. Zhang et al., (2010), has recently published a work about the flow pattern transition and the break-up mechanisms of liquid film in

single-channel *FFMR* while Al-Rawashdeh et al., (2008), have numerically investigated the effect of liquid flow distribution, gas chamber height and hydrophilic-hydrophobic channel material. To the authors best knowledge only Yeong et al., (2006) have experimentally investigated the shape of the interface and the liquid film thickness using laser scanning confocal microscopy.

The design and production time for complex microreactors is considerably long (Klank et al., 2002) and thus it is important to be able to predict the flow phenomena as well as the parameters that affect the operation of such systems. This work is part of a project that concerns the study of flow characteristics in microchannels. The aim of this study is to investigate the effect of liquid phase properties and channel dimensions on the characteristics of the liquid film. For this purpose a non-intrusive measuring technique (*μ-PIV*) is employed for acquiring the geometrical characteristics of the falling film and reconstructing the shape of the interface.

2. Experimental procedure

The development of reliable non-intrusive methods for liquid film measurements is very important in the area of multiphase flow. However, not all the methods that are suitable for applications in macroscale, can be applicable in the microscale. For example, the use of special probes (like electrodes) mounted to the channel walls might not be feasible in the microscale, while the small liquid volume might render the generated signals too weak to be successfully detected and measured. Micro Particle Image Velocimetry (*μ-PIV*), which is a common optical non-intrusive technique for measuring two-dimensional velocity fields, is used in this work. In the present study, this method is also employed for estimating the thickness of the liquid phase and defining the shape of the interface. The *μ-PIV* method is based on the imaging of tracing particles (**Figure 1a**) that accurately follow the flow. For each measurement two successive particle images must be acquired over a known time interval, Δt. These images are divided into

smaller regions called interrogation areas. By employing in every interrogation region cross correlation techniques the displacement of a group of particles is determined. The local velocity is calculated from the estimated displacement (ΔS) and the time interval (Δt). Combining the data from each interrogation region a two-dimensional vector map of the flow is obtained (**Figure 1b**).
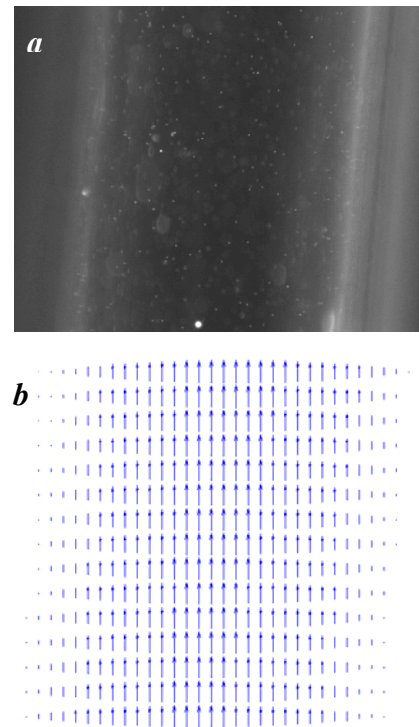

Figure 1: The process of a μ-PIV measurement; a) One of the two initial images of the flow showing the tracing particles; b) Two-dimensional vector map.

As the dimensions of the systems investigated are in microscale the flow should be imaged with sufficiently high magnification and with high diffraction resolution optics. For this reason a microscope and appropriate objective lenses are used. The most common microscope objective lenses range from diffraction-limited oil-immersion lenses with magnitude (*M*) equal to 60x, and numerical aperture (*NA*) equal to 1.4 to low magnification air-immersion lenses with *M=10x* and *NA=0.1*. From these technical characteristics important parameters such as the spatial resolution and the depth of field or more appropriately the depth of the correlation are defined. The depth of field refers to the distance a point source of light may be away from the focal plane and

still produce an acceptably focused image, whereas the depth of correlation refers to how far from the focal plane a particle will contribute significantly to the correlation function (***Figure 2***). The narrower the depth of correlation the more detailed velocity profiles can be obtained. This can be achieved by varying the height at which microscope is focused and by taking measurements on many planes. Taking advantage of the narrow depth of field, which permits focusing and taking measurements on different planes, the gas-liquid interface can be recognized and the shape of the interfacial area can be reconstructed.

To conduct the measurements, the liquid phase is seeded with light emitting particles. In this case gas/liquid interface can be easily distinguished on an image of the flow conduit (***Figure 3a***). The dark region between the two groups of particles is the gas phase, while the outer dark regions correspond to the walls of the microchannel.
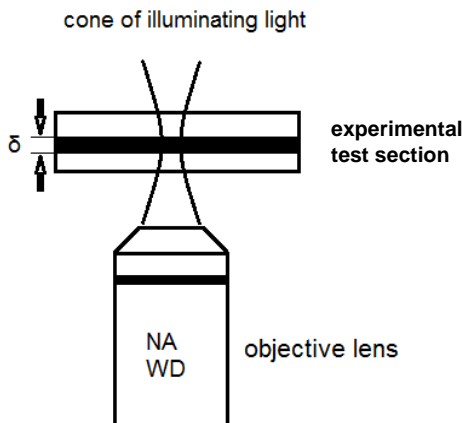
Figure 2: Depth of field (*δ*) of an objective lens.

The distance between the wall and the gas phase is the width of the liquid phase (***W***). The top of the interface coincides with the plane where the first particles can be recognized (*plane A* at ***Figure 3b***). At this point the liquid phase covers a very narrow region (***Figure 3a***). As the focusing plane is moving closer to the bottom wall (e.g. ***Figure 3***, intermediate planes), with a step of 10μm, this region broadens until the point where the two liquid regions are close to merge. The first plane where only the liquid phase can be observed is recog-

nized as the end point of the gas-liquid interface. As the flow is laminar and the concept of continuity is valid a three-dimensional vector field can be reconstructed by combining the data obtained from each plane (Meinhart, 2007).
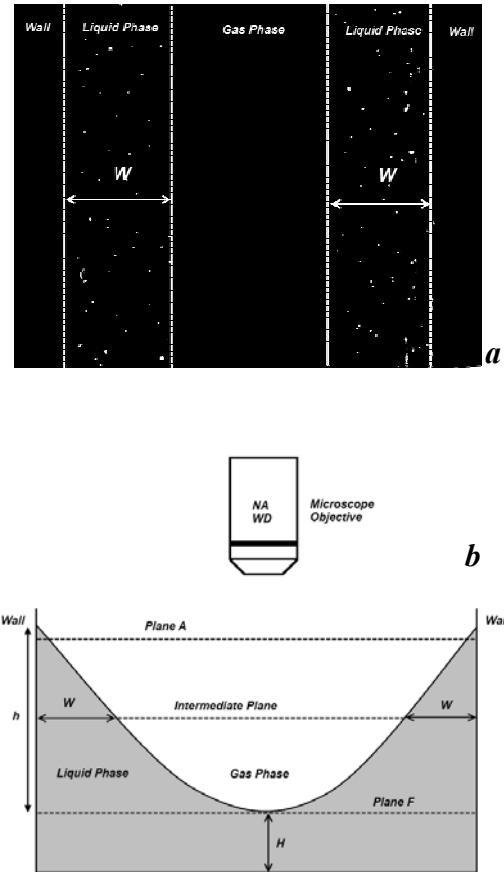
Figure 3: a) Typical μ-PIV image corresponding to the intermediate plane; b) Schematic of the microchannel showing the various measuring planes.

In ***Figure 4*** the forces that influence the liquid flow are presented. The downward force F_b is a function of the liquid density (***ρ***), inclination angle (***φ***) and the acceleration of gravity (***g***). The forces ($F_σ$) due to the surface tension and (F_w) due the wall shear stress are both upward forces that impede liquid movement. Consequently, to understand the mechanism of liquid film formation in microscale the parameters (i.e., surface tension, density and viscosity of the liquid phase) that affect the magnitude of the aforementioned forces must be considered.
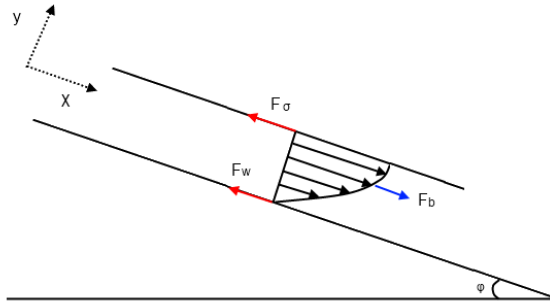
Figure 4: Force balance in free flow liquid.

3. Experimental setup

The experimental setup (***Figure 5***) consists of a fluorescent *μ-PIV* system, the test section of the microchannels and a syringe pump for generating the flow.
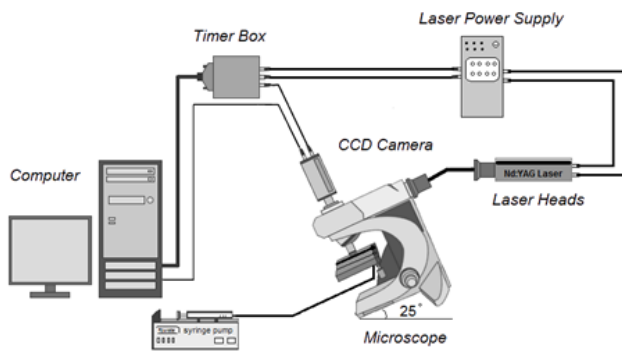

Figure 5: Experimental setup.

The experiments were conducted in three square cross section microchannels having a length of 1200mm and three different widths (D_1=1200μm, D_2=600μm, D_3=300μm). The test section (***Figure 6***) is constructed by high accuracy micromachining techniques on polymeric material. In order to assure continuous free flow, the liquid phase enters by overflowing a circular region preceding the inlet of each microchannel.

The measuring section of the micro channel was illuminated by double cavity laser emitting at 532nm. The flow was recorded using a high sensitivity *CCD* camera, connected to a *Nikon* (*Eclipse LV150*) microscope. The light source, a laser emitting at 532nm, was synchronized with the camera shutter by a timer box. The flow was traced by adding fluorescent polystyrene particles with mean diameter of 1μm. In order to obtain magnified images a 20X air immersion objective with *NA*=0.20

was used and this corresponds to 8μm depth of correlation. The time delay between frames lies in the range of 150-1500μs, depending on the flow rate studied each time, while the sampling rate was *5Hz*. The vector maps were estimated by averaging 100 images acquired for each measurement. The Flow Manager Software (*DantecDynamics®*) is employed for processing the images and estimating the velocity.
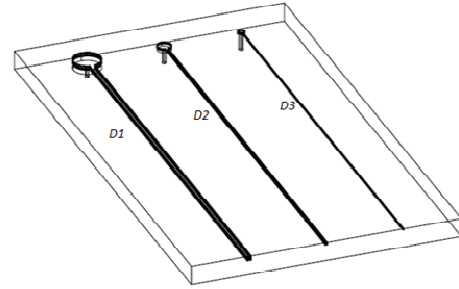

Figure 6: The test section (D_1=1200μm, D_2=600μm, D_3=300μm).

All the liquids employed, namely aqueous solutions of glycerol and butanol as well as water used as reference, exhibit Newtonian behavior. The properties of the liquids used, i.e the density ($ρ$), the surface tension ($σ$) measured by a tensionmeter (*Cam200 optical contact angle meter*), and the viscosity ($μ$), measured with an Oswald viscometer, are presented in ***Table 1***.

Table 1: Physical properties of the fluids used.

index	liquid	$μ$, (cP)	$ρ$, (kg/l)	$σ$, (mN/m²)
w	**Water**	1.00	0.99	72.0
g-1	**Glycerol 20%w/w**	1.80	1.03	70.8
g-2	**Glycerol 30%w/w**	2.30	1.07	69.0
b	**Butanol 2%v/v**	0.98	0.99	49.0

The test section was placed at an inclination angle of 25 degrees from the horizontal position. To eliminate entrance phenomena all the measurements were performed 40mm downstream from the inlet of the micro-channels. The flow was generated by a syringe pump (*ALLADIN 2000*).

4. Results and discussion

Depending on the liquid flow rate, three different shapes of interface are encountered (***Figure 7a***). At lower flow rates a meniscus is

formed (*Figure 7a-left*), as it is expected considering the hydrophilicity of the microchannel material (*contact angle* 62º) and the great effect of capillary forces in such small conduits. By increasing the liquid flow rate the meniscus height (*h*) (as defined in *Figure 3b*) decreases and the interface becomes flat (*Figure 7a-centre*). For even higher flow rates the liquid interface is slightly raised at the center of the micro channel (*Figure 7a-right*). It must be noted in the case of solutions *g-1* and *g-2* a flat interface is formed for flow rate values lower than that of liquids *b* and *w* (*Figure 7b*). By comparing these shapes, it is obvious that, for a given liquid cross-section the presence of a meniscus extends the size of the gas-liquid interfacial area.
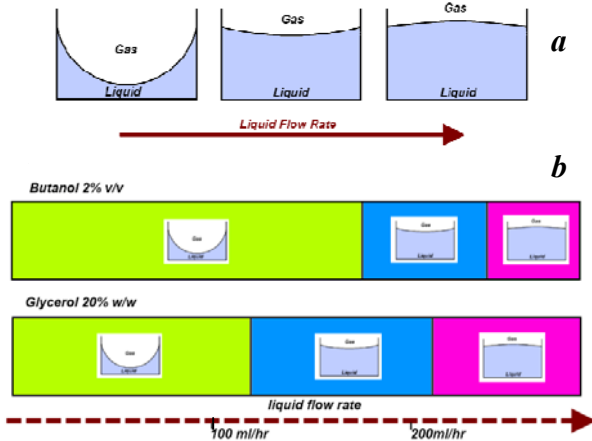
Figure 7. a) The different shapes of the gas-liquid interface; b) Comparison of the interface shape between *b* and *g-1* for D=1200μm.

By combining the liquid phase width (*W*) measurements on consecutive planes the shape of the interface can be reconstructed and its extent can be estimated (*Figure 8*). In Figure 8a the shape of the interface for the case of liquid b and for various mass flow rates normalized with respect to the channel width ($m_N = m/D$) is presented, while the x-axis is the width (*d*) normalized with respect to the total microchannel width (*D*). It is obvious that the height of the meniscus (*h*) is greater for the lower flow rates employed. In *Figure 8b* the shape of the interface for three different liquids (*b*, *g-1* and *w*), and for the same m_N values is shown. It can be observed that the more viscous liquid (*g-1*) forms shorter meniscus

comparing with liquids *b* and *w*. Using these measurements the extent of the interface can be also estimated. For example it was found that when the water flows in the 1200μm channel the existence of a meniscus provides 29% greater interfacial area compared to that of a flat surface. Thus it would be desirable to operate the *FFMR* in conditions that ensure the formation of a meniscus in the case that extensive interfacial area is required.
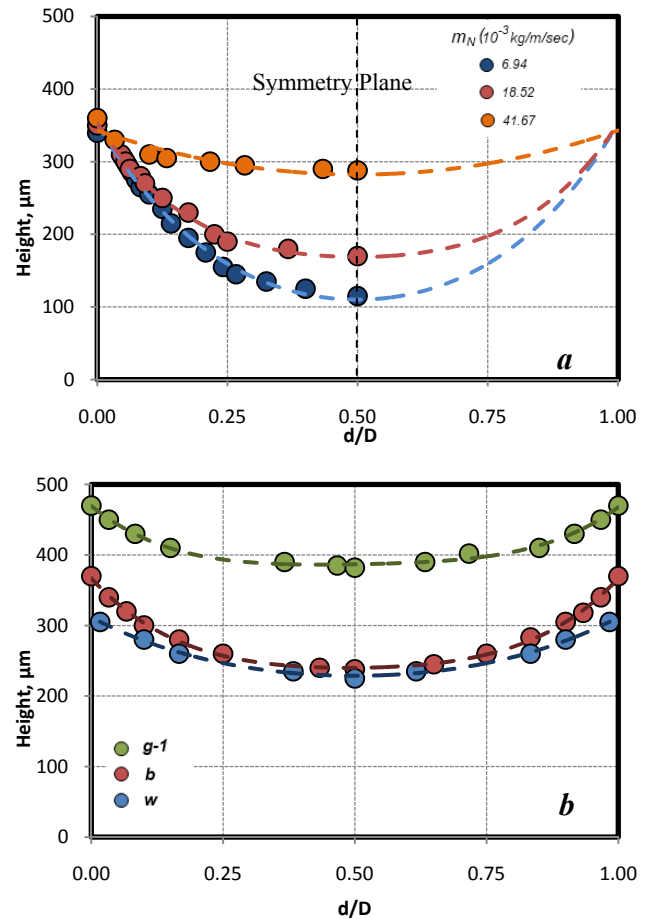
Figure 8. Reconstruction of the gas liquid interface from the μ-PIV measurements as a function of the channel width normalized with respect to the total width of the microchannel a) Liquid *b* for three different flow rates and D=1200μm; b) Comparison between *w, b and g-1* for m_N= 13.89 10^{-3} kg/m/sec and D=600μm.

Using the same experimental set-up the thickness *(H)* of the liquid phase (*Figure 3b*) was also measured with the following procedure. Starting from the last plane of the interface (*plane F, Figure 3b*) the focusing plane is moved towards the bottom wall of the channel with a step of 10μm, until no particles are observed. This is regarded as the bottom of the microchannel and hence the distance

measured is the thickness **(H)** of the liquid phase.

In **Figure 9** the liquid film thickness versus the normalized mass flow rate **(m_N)** is presented for three different liquids and for D=1200μm. It is obvious that, although butanol (**b**) and water (**w**) exhibit almost identical behavior, the more viscous glycerin solution (**g-2**) produces thicker liquid films especially for the greater **m_N** values applied.
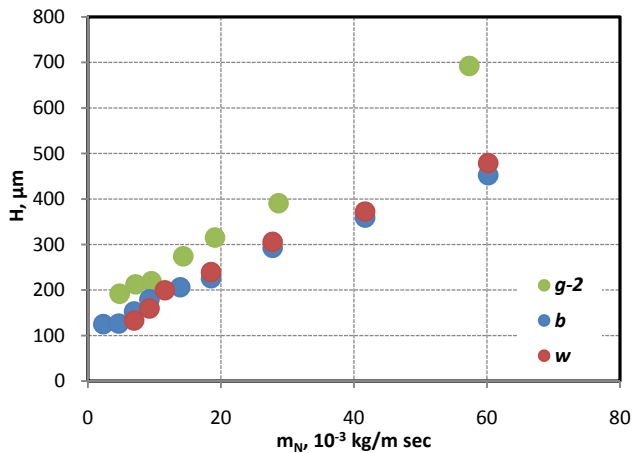
Figure 9: Liquid film thickness (D=1200μm).

In **Figure 10** the effect of liquid flow rate on film thickness is presented for all liquids employed and for D=600μm. Up to a **m_N** value of 10g/m/sec, the liquid film thickness is practically the same regardless of the liquid, while for higher **m_N** values the glycerin solutions give much thicker films.
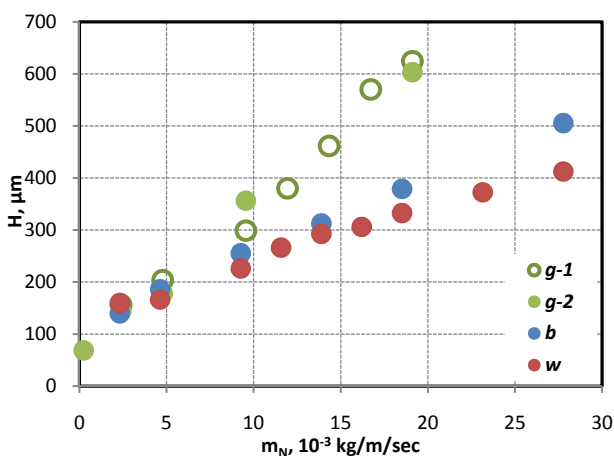
Figure 10: Liquid film thickness (D=600μm).

It is also worth noticing that for **b** and **w** the film thickness is practically the same, denoting that for this channel dimension the effect of

surface tension is negligible.

In **Figure 11** the effect of liquid properties on film thickness (**H**) is illustrated for the 300μm microchannel. It must be noted that this microchannel can operate only for very low flow rates, because an increase of feed rate causes the liquid to overflow. As before, the more viscous the liquids the thicker the film measured. Another observation is that in such narrow conduits the surface tension seems to play a more significant role, as the liquid with the lowest surface tension (**b**) generates the thinner films.
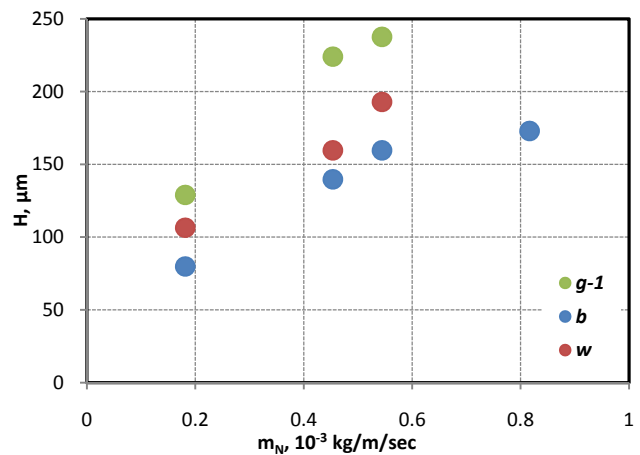
Figure 11: Liquid film thickness (D=300μm).

In **Figure 12** the effect of the channel width on the film thickness (**H**) is presented. It is clear that, for a given flow rate (**m_N**), the liquid film thickness increases considerably when the channel width is reduced. This difference is more pronounced for the higher flow rates employed. The same behavior was observed for all the liquids studied. It is noted that for the 300μm microchannel rather thick films are generated even for very low mass flow rates, thus these data are not included in **Figure 12.**

Finally, in **Figure 13** the experimental data are compared with the values predicted by the widely used *Nusselt* correlation:

$$H_{Nu} = \left(\frac{3v^2 Re}{g\sin\theta}\right)^{1/3} \qquad (1)$$

The various results presented in **Figure 13** are normalized with respect to the corresponding H_{Nu}. It must be noted that the aforementioned correlation assumes that both the side walls

and the surface phenomena have no effect on the liquid film characteristics. Obviously, and given the dimensions of the conduits employed, this assumption cannot hold true in the present study.
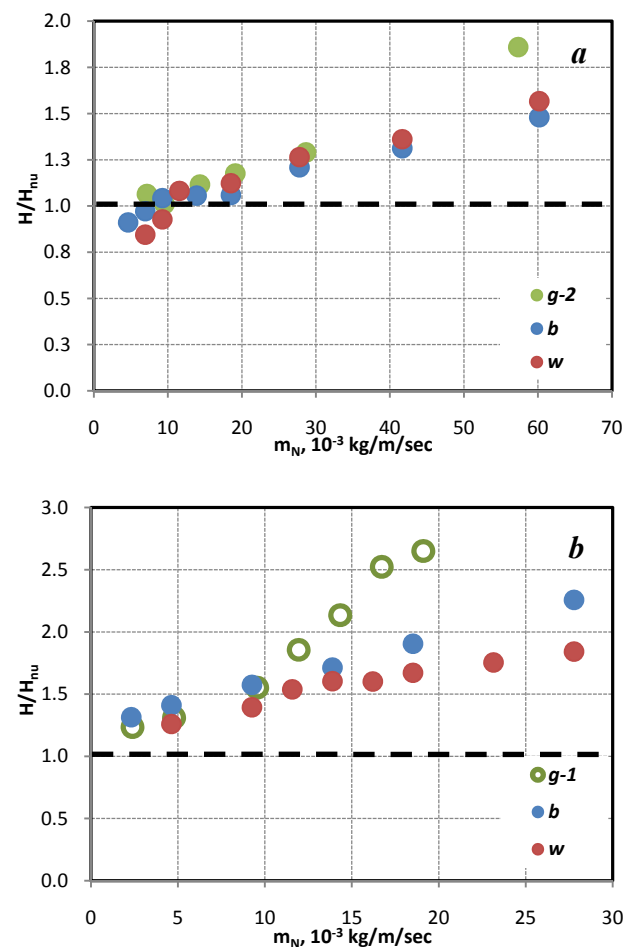
Namely, in *Figure 13a* (for D=1200μm) it is obvious that for low mass flow rates (up to 10g/m/sec) and regardless of the liquid used, the correlation overestimates, whereas for higher flow rates underestimates the film thickness. On the other hand for D=600μm (*Figure 13b*) the correlation is unable to predict film thickness with reasonable accuracy even for low liquid flow rates.

the film thickness (**H**) at the bottom also increases while the height of the meniscus (**h**), (*Figure 3b*) remains relatively unchanged, rendering the presence of the meniscus less important. On the other hand as the width of the microchannel becomes smaller both the drag forces exerted by the walls and the surface phenomena become more significant. This hinders the flow of the liquid phase and consequently increases its volume and thickness. It is obvious that under these circumstances correlations valid in macroscale underestimate the thickness of the liquid film up to 170%.
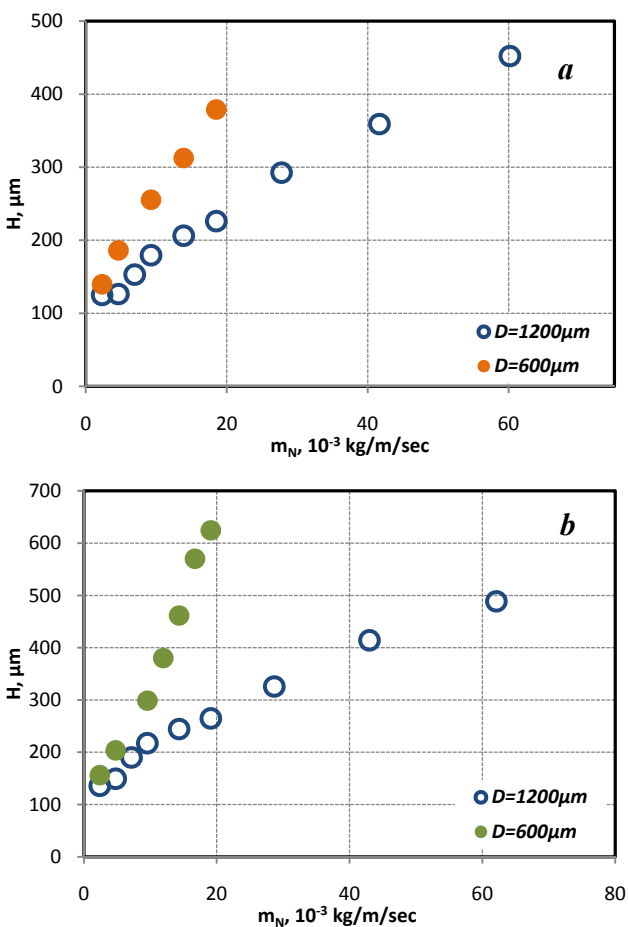
Figure 12: Effect of channel width on liquid film thicknes *H*. a) solution *b*; b) solution *g-1*.

Figure 13: Comparison between experimental results and theoretical correlations as a function of the normalized mass flow rate. a) D=1200μm; b) D=600μm.

These findings can be explained by considering the relevant magnitude of the forces acting on the liquid phase. At the larger microchannel the effect of the walls is not so important and the difference between experimental results and correlations can be attributed to the existence of the meniscus. As the flow increases,

5. Conclusions

The scope of this work was to study the characteristics of the liquid phase in a *FFMR* using a *μ-PIV* system. Experiments were conducted in three microchannels (D=1200μm,

600μm and 300μm) and for Re in the range of 0.9 to 39.7. It was confirmed that, as the capillary forces become important in such narrow conduits, the liquid film tends to form a meniscus especially for the lower flow rates employed. The comparison of the experimental results with an expression valid in macroscale proved that, as it was expected, such correlations are not generally valid in the microscale.

It is obvious that the presence of a meniscus considerably increases the interfacial area available for gas-liquid reaction in *FFMR*s. As the liquid flow rate increases the meniscus turns to disappear till the interface becomes flat and finally even slightly raised at the center. The meniscus is also more pronounced for the lower viscosity liquids tested. It was also proved that the geometrical characteristics of the liquid film are not considerably affected by the surface tension. However, when the channel width is reduced the contribution of surface tension turns to be more significant.

In conclusion and in order to be able to design more efficient *FFMR*, it would be very useful to be able to predict the geometrical characteristics of the liquid film as a function of both the physical properties of the fluid and the geometrical characteristics of the conduit. Certainly, more work is needed and indeed is currently in progress in order to be able to assess the relative importance of all the parameters that are involved in the design of a *FFMR*. The ultimate goal would be to formulate reliable design equations valid in the microscale.

Notation

D	Total microchannel width, μm
d	Microchannel width, μm
F_b	Body force, N
F_w	Wall shear stress, N
F_σ	Surface tension force, N
g	Acceleration of gravity, m/s^2
H	Liquid film thickness, μm
H_{Nu}	Nusselt's liquid film thickness, μm
h	Height of the meniscus, μm
M	Objective lenses magnitude
m_N	Normalized mass flow rate (m_N=m/D), $kg/m/s$
m	Mass flow rate, kg/s (g/s)
NA	Numerical aperture
W	Width of liquid phase, μm
w	Water

Greek Symbols

μ	Liquid viscosity, $mPa\ s$
σ	Surface tension, N/m
ρ	Liquid density, $kg/m^3\ g/ml$
φ	Inclination angle, $degrees$

REFERENCES

Al-Rawashdeh, M.m., Hessel, V., Löb, P., Mevissen, K., Schönfeld, F., 2008. Pseudo 3-D simulation of a falling film microreactor based on realistic channel and film profiles. Chemical Engineering Science **63**, 5149-5159.

Chambers, R.D., Holling, D., Spink, R.C.H., Sandford, G., 2001. Gas - liquid thin film microreactors for selective direct fluorination. Lab on a Chip **1**, 132-137.

Chasanis, P., Lautenschleger, A., Kenig, E.Y., 2009. CFD-based investigation of carbon dioxide absorption in a falling-film micro-absorber. Chemical Engineering Transaction **18**, 593-598.

Klank, H., Goranovic, G., Kutter, J.P., Gjelstrup, H., Michelsen, J., Westergaard, C.H., 2002. PIV measurements in a microfluidic 3D-sheathing structure with three-dimensional flow behaviour. Journal of Micromechanics and Microengineering **12**, 862-869.

Meinhart, C.D., 2007. A 3D-3C Micro-PIV Method, Conference on Nano/Micro Engineered and Molecular Systems, Bangkok.

Nguyen, N.-T., Wereley, S.T., 2002. Fundamentals and Applications of Microfluidics: Second Edition. Artech House, Boston.

Stavarek, P., Le Doan, T.V., Loeb, P., De Bellefon, C., 2009. Flow visualization and mass transfer characterization of falling film reactor. Proc. 8th World Congress of Chemical Engineering, Montreal, Canada.

Yeong, K.K., Gavriilidis, A., Zapf, R., Kost, H.J., Hessel, V., Boyde, A., 2006. Characterisation of liquid film in a microstructured falling film reactor using laser scanning confocal microscopy. Experimental Thermal and Fluid Science **30**, 463–472.

Zhang, H., Yue, J., Chen, G., Yuan, Q., 2010. Flow pattern and break-up of liquid film in single-channel falling film microreactors. Chemical Engineering Journal 163, 126-132.

Ziegenbalg, D., Löb, P., Al-Rawashdeh, M.m., Kralisch, D., Hessel, V., Schönfeld, F., 2010. Use of `smart interfaces' to improve the liquid-sided mass transport in a falling film microreactor. Chemical Engineering Science **65**, 3557-3566.